JOURNAL OF OPTOELECTRONICS AND ADVANCED MATERIALS Vol. 12, No. 3, March 2010, p. 783 - 788

Treatment of aluminium foil by laser interference metallurgy for selective etching

M. D'ALESSANDRIA*, F. MÜCKLICH
Department of Material Science, Institute of Functional Materials, Saarland University, Campus D3.3, room 2.07, P.O. Box 15 11 50, D-66123, Saarbrücken, Germany

In the preset work the site-controlled formation of the etch pits in aluminium foil modified by laser interference metallurgy (LIMET) is investigated. The principle of this technique is the fabrication of periodic patterns based on a spatial variation of the intensity created by the interference of several laser beams. Ordered local passivation and/or activation, this last promoted by the introduction of a small amount of lead on the aluminium foil, permit the selective etching of an exposed aluminium surface. By controlling the etching process, a better distribution of the etch pits can be achieved which may ultimately lead to an increase of the total surface area. The obtained ordered array of etch pits can be used to the improvement of electrolytic capacitors, which use surface-enlarged aluminium foil as electrode.

(Received June 19, 2009; accepted January 18, 2010)

Keywords: Laser interference, Selective etching, Aluminium

1. Introduction

Significant works have demonstrated the use of pulsed laser sources for the modification of material surfaces, such as melting, phase transformations, hardening, oxidation, thin film deposition, micro-structuring, etc. [1-5]. One of the advantages of employing short pulsed lasers is that they allow the modification of the surface morphology and/or structure without significant damages or alterations to the underlying material. This characteristic made them an attractive tool for the modification of anode aluminium foils for high voltage capacitor applications. An aluminium electrolytic capacitor consists of an anode foil on which an oxide is formed (dielectric), a suitable electrolyte and a cathode foil. In principle, a high capacitance device requires a large surface area of the anode foil. Formation of tunnel pits on aluminium by anodic etching in an electrolyte containing Cl^- anions has been extensively employed for the increase of the surface area. By etching the aluminium surface, the effective surface area of the foil as compared to the apparent area can be enlarged 30-40 times for high voltage capacitors. The etching process is typically carried out via electrochemical etching, and results in the formation of a great number of micron-wide corrosion tunnels which follow the ⟨100⟩ crystallographic direction in aluminium. For the purpose of obtaining the maximal possible capacitance, the tunnel pits should be evenly distributed on the surface, and their size and interval must be precisely controlled [6-8]. Multiple factors such as, grain size, cubic texture (proportion of cubic grain having (100) orientation), uniformity of the oxide layer, concentration impurity and/or pre-treatments can influence the tunnel etching [9-13]. In general, the grain size of aluminium foil for high voltage capacitors is very large, ca. 50 ~ 200 μm. High cubic texture fraction (*cubicity*) are important because it has been shown that tunnels are formed preferentially along the ⟨100⟩ direction in hydrochloric acid. The effect of impurity elements, such as Fe, Cu, Mn, Zn, Pb, etc., present in aluminium foil at ppm levels, are applied to increase the number of tunnel pits so as to enhance etchability.

A great number of studies are in progress which try to better understand the formation and control of the pit-site distribution during the DC anodic etch process of aluminium foil. In the present work, the influence of "Laser Interference Metallurgy" as well as the effect of lead on the site-controlled pitting during the chemical etch process is investigated. Laser Interference Metallurgy (LIMET) allows the formation of a stationary spatial variation of the intensity created by the interference of several laser beams. The pattern that emerges out of the intensity distribution is transferred to the material surface by means of photo-thermal mechanisms [14, 15]. The structuring of the samples is carried out using a pulsed *Nd:YAG* laser. Lead (Pb) addition is performed by a physical vapour deposition (PVD) process. The characterization of the systems is carried out by SEM and TEM analysis.

2. Experimental

The samples consisted of high-purity, annealed, and degreased aluminium foil for high voltage electrolytic capacitor applications. The surface of the specimen is

composed predominantly of (100) planes. The thickness of the foil was 120 μm approximately. Additionally, a series of lead-enriched samples were prepared. A thin film of lead was deposited on aluminium foil using non-reactive physical vapour deposition (PVD). The lead layer thickness was approximately 10 nm.

A high power pulsed *Nd:YAG* laser was used for laser interference experiments. The laser patterning was carried out using a wavelength λ of 355 nm, a frequency of 10 Hz and a pulse time τ of 10 ns. In all the cases, a mechanical shutter was employed to select single pulses. A square-shaped mask was used obtaining a final beam size of 2.3 mm × 2.3 mm. The structuring of the samples was performed by splitting the output beam into two or three coherent beams of equal intensity, which coincide on the samples surface under an incident angle (2θ). Inherent periodicity in the laser intensity is transferred to the material yielding the micro-structures. In general, the interference of two and three coherent laser beams results in one and two dimensionally periodic patterns. The interference of two beams produces a linear pattern whose grating period (d) is related with λ and the incident angle by:

$$d = \frac{\lambda}{2\sin(\theta)} \tag{1}$$

If three laser beams arranged symmetrically are used, a hexagonal dot interference pattern is obtained, whose period is given by:

$$d = \frac{\lambda}{\sqrt{3}\sin(\theta)} \tag{2}$$

All the samples, the pristine aluminium foil and the Pb (10 nm)/Al systems, were irradiated under atmospheric conditions. The grating period was varied by changing the angle between the beams.

In order to study the influence of LIMET on the control of pit initiation sites on aluminium and Pb (10 nm)/Al, the specimens were exposed to hydrochloric (HCl) solution at 85°C. The etch time was 5 s. The chemical and not electrochemical etching was chosen to preserve the laser trace on the sample surface after the etching process. The surface morphology of etched aluminium foils was studied using scanning electron microscopy (SEM). Finally, TEM lamellae were prepared with the aid of a dual beam workstation, consisting of a focused ion beam (FIB) used for site-specific milling, and a scanning electron microscope (SEM) to image the samples. TEM examinations of the structured samples were carried out using a Jeol JEM 200 CX.

3. Results and discussion

SEM surface analyses of pristine and laser structured samples are shown in Fig. 1. Aluminium foil in the original condition reveals an abrupt surface composed of thin and directional grooves coming from the previous rolling process (Fig. 1a). The structuring of Al was carried out employing different laser configurations. Fig. 1(b, c) show the line- and dot-like patterns created on Al using the interference of two and three beams, respectively. The selected laser fluences, F, were 688 mJ.cm^{-2} and 1100 mJ.cm^{-2} for line and dot patterns respectively. The zones of maximal (Max.) and minimal (Min.) interference are indicated. At these fluence values a small portion of the material is molten at the maximal interference positions while at the minimal interference positions, the characteristic grooves of the unmodified surface can still be observed. Independently from the pattern shape, the material is always removed from the interference maxima to the interference minima. The quantity of molten material depends on the laser fluence employed. By increasing the fluence, more energy is absorbed by the material [16] and the temperature at the energy maxima increases. Consequently, a larger volume of material is molten [15]. As the surface tension of aluminium decreases with the temperature [17], molten aluminium tends to pull away from the hotter regions (interference maxima) toward the cooler regions (interference minima) producing the surface deformation (known as Marangoni effect or surface-tension-driven convection) [17, 18]. When the fluence further increases, the molten material coming from two neighbouring maxima positions meets at the minimum position located between them, leading to the creation of a band of re-solidified material, to produce the compact structures. Fig. 1 (b) and (c) show surface topographies of the samples structured using relatively low fluences. A detailed analysis of the formation mechanism of the periodic patterns is present in [15].

Moreover, SEM analysis of aluminium coated with lead shows a relatively denser layer with "cauliflower" morphology, typical of PVD coatings (Fig. 1(d)). Pb/Al samples were structured using similar conditions as for aluminium foil. Fig. 1(e, f) show the morphology of Pb/Al structured with two laser beams creating line- and grid-like patterns. The grid pattern was built up by producing two consecutive linear patterns and rotating the sample 90° after the first line pattern (Fig. 1(f)). The laser fluences and grating distances employed were F=420 mJ.cm^{-2}, d=4.5 μm and F=953 mJ.cm^{-2}, d=10 μm for linear and grid patterns, respectively. Depending of F and d used, the lead layer at the minima position can be melted or not. Fig. 1(e) reveals the re-solidified lead at the minima zones whereas

in Fig. 1(f) the lead layer remains at the minima positions without visible superficial changes.

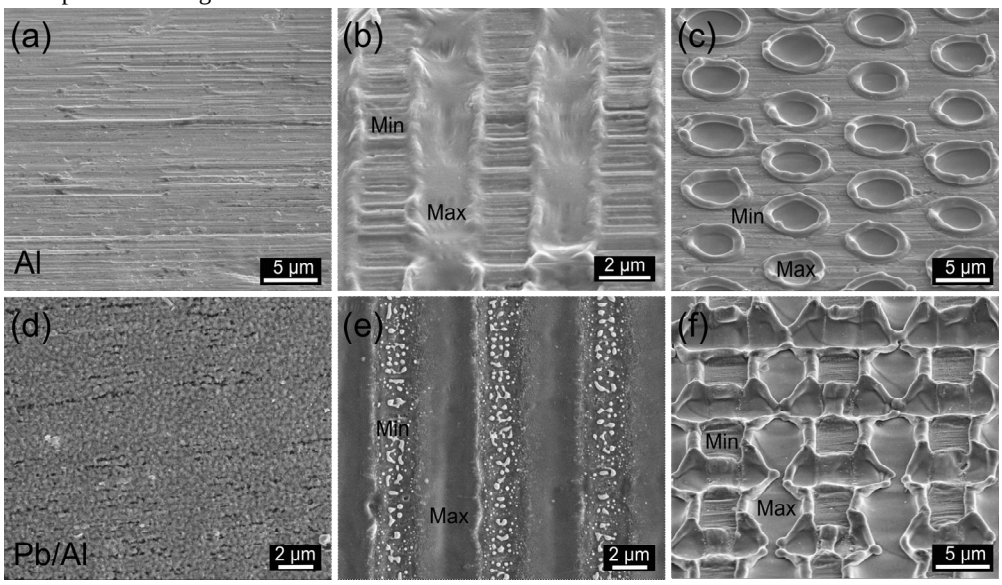

Fig. 1. SEM images of (a-c) aluminium and (d-f) lead/aluminium samples. (a) Original surface condition of Al. (d) As-coated Pb/Al. (b-c, e-f) Periodical structures created on Al and Pb/Al by laser interference irradiation producing (b,e) line-, (c) dot-, and (f) grid-like patterns. Tilt 52°.

Additionally, TEM investigations of the non-irradiated and structured Al samples were carried out. Firstly, the native oxide layer thickness of the Al foil was determined, by TEM, to be $5.2^{\pm 0.8}$ nm thick, approximately. Figure 2(a) shows the TEM lamella created perpendicularly to the line structures formed on Al surfaces using a grating distance of 4.5 µm and 1015 mJ.cm^{-2} laser fluence. It was found that besides the formation of periodic structures, laser interference also produced a local thermal reaction on the sample. At 1015 mJ.cm^{-2}, almost compact line structures (Fig. 2(a)) are created where the maximal and minimal interference positions can be easily recognized. The first energy minimum from left to right is almost completely formed, and only a small porosity remains as a consequence of the material displacement from the two neighbouring maximal to the minimal interference zones. The second energy minimum clearly shows the motion of molten material due to the Marangoni effect. According to TEM results, local and periodic oxidation took place during laser structuring. An oxide layer was found with a measured thickness of $10.1^{\pm 1.4}$ nm at maximal (Fig. 2(b)) and $6.2^{\pm 0.2}$ nm at minimal (Fig. 2(c)) interference positions. The oxide layer produced during laser irradiation demonstrated to be quite dense and homogenous. Similar investigations were performed for Al structured at different laser fluences and it was determined that the oxide layer thickness increases with the laser fluence and in all cases the thickness at the maxima is greater than that at the minima. An accurate investigation of the chemical behaviour of aluminium modified by laser interference is developed in [19]. However, the thermal effects alone cannot explain the oxidation by laser. There are other parameters, such as feedback and electronic effect, which play important roles during laser induced oxidation [20, 21].

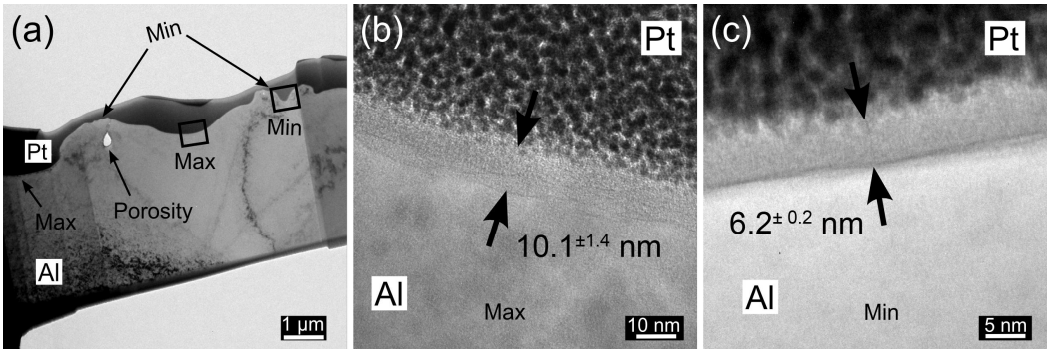

Fig. 2. TEM investigation of the oxide layer formed during laser structuring of Al foil. The laser fluence used was 970 mJ.cm^{-2}. (a) TEM lamella showing the maximal and minimal interference positions; (b-c) high magnifications of oxide layer thickness at the maximal and minimal interference zones, respectively.

Similar TEM analyses were performed for Pb/Al structured samples. Figure 3(a) exhibits the structured Pb/Al TEM lamella created perpendicular to the line-like patterns using d=4.5 µm and 1600 mJ.cm^{-2} laser fluence. Figure 3(b-d) revealed the presence of some lead nanoparticles at the oxide-metal interface which are essentially concentrated toward the oxide side of the oxide-metal interface. Furthermore, some lead inclusions were revealed by TEM, as was expected considering the low solubility of lead in aluminium [22]. The lead-enrichment of aluminium is assisted by LIMET. Because the main mechanism to create micro-structures is the surface-tension gradient induced by lateral variations of the temperature (Marangoni convection), LIMET promotes the incorporation of lead particles in aluminium foil. It can also be observed that during the Pb/Al patterning, the transient oxidation decreases in comparison to the oxidation found during the structuring of aluminium samples in absence of lead (see Figs. 2 and 3).

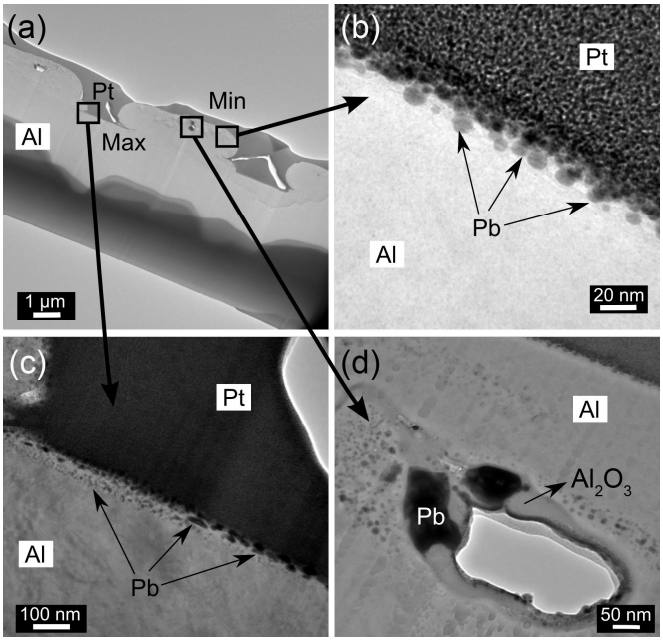

Fig. 3. (a) TEM lamella of Pb/Al samples structured at 1600mJ.cm^{-2}. (b-d) Incorporation of lead nanoparticles at the oxide layer and metal-oxide interface at the minimal (b,d) and maximal (c) interference zones.

For the purpose of finding the effect of laser structuring and lead on the chemical behaviour of aluminium foil, the samples (Al and Pb/Al) were exposed to 1N HCl solution at 85°C after laser structuring (Fig. 4). In both systems studied, Al and Pb/Al, a selective etching was found. In both cases the samples show a precise, localized and periodic etch but in different zones. The etched Al surface shown in Fig. 4(a, b) reveals that the etching occurs preferentially at the interference minima zones due to the difference in oxide layer thickness between the maxima and minima positions. The thin oxide layer built up during laser structuring enhances the chemical stability of the irradiated zones. The initial pit-sites occur at the minima positions because the oxide formed at the maxima is thick enough to protect the metal from the etchant at the beginning of the corrosion process. However, at high laser fluences, the whole surface becomes passive. We estimate that when the oxide layer thickness reaches or exceeds 10 nm, the surface becomes completely passive.

It is very interesting to observe how the behaviour of the etching process totally changes with the presence of lead. Aluminium foil covered with a thin lead layer, (Pb/Al), and structured with laser shows also a preferential etching (Fig. 4(c, d)), but in this case, in the energy maxima zones, i.e., where the surface was irradiated. At the energy maxima positions, aluminium foil reveals an activation of its surface induced by lead. The chemical activation of aluminium requires the wetting of aluminium with lead, also in metallic form. This conclusion comes from etching of Pb/Al samples structured at a laser fluence value adequate to produce only the local removal (ablation) of the lead layer at the maxima positions (this state is not represented in Fig. 4). In these conditions, the preferential etching of the samples did not occur. Therefore, the local and preferential etching of Pb/Al

samples (Fig. 4(c, d)) take place only when the Pb particles remain in contact with the aluminium metal (Fig. 3(b-d)). The nonwetting Pb particles in the oxide layer did not contribute to the surface activation of aluminium. The occurrence of a metallic Pb enrichment at the metal-oxide surface must have a significant destabilizing effect on the passivity of the Al oxide film, thereby causing surface activation combined with the synergistic destabilizing role of the Cl^- chloride ions in the solution [23].

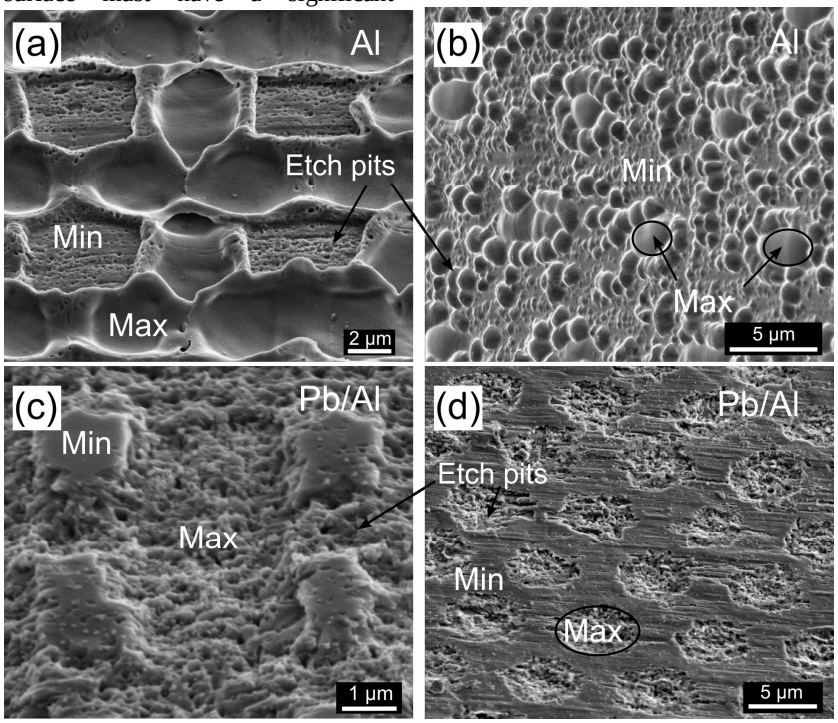

Fig. 4. SEM images of structured Al and Pb/Al surfaces after chemical etching. Independently from the laser configuration used, grid- (a,c) and dot-like patterns (b,d), the selective etching occurs: at the minimal interference positions for structured aluminium (a-b), and at the maxima for Pb /Al (c-d).

Finally, the lead addition promotes the development of refined pits with a regular distribution in comparison to these one found during the etching of Al samples without Pb. Independently from the laser configurations employed, grid- (Fig. 4(a, c)) or dot-like patterns (Fig. 4(b, d)), a selective etching takes place following the ordered arrays imprinted by laser interference.

4. Conclusions

This study demonstrates that Laser Interference Metallurgy is a promising process for the improvement of the site-controlled pit etching of aluminium foils. This technique permits to control the growth of a periodical and defined oxide layer on aluminium. The oxide layer built up by laser irradiation enhances the stability of irradiated zones. The difference in oxide layer thickness between the maxima and minima positions leads to a preferential and local etching of Al samples at the minimal interference positions. Additionally, the combination of lead and LIMET produces anodic activation of the aluminium surface as a result of the enrichment with lead nanoparticles predominantly in the oxide-metal interface, causing passivity breakdown. In this case the preferential etching takes place at the maximal interference positions. In both systems studied, the etching process follows the ordered array imprinted on the surface via LIMET.

References

[1] T. Dimogerontakis, R. Oltra, O. Heintz, Applied Physics A: Materials Science and Processing **81,** 1173 (2005).
[2] G. Kerner, M. Asscher, Surface Science **557,** 5 (2004).
[3] A. Pérez Del Pino, P. Serra, J. L. Morenza, Applied Surface Science **197-198**, 887 (2002).
[4] J. Zhu, G. Yin, M. Zhao, D. Chen, L. Zhao, Applied Surface Science **245,** 102 (2005).
[5] K. Dou, R. L. Parkhill, J. Wu, E. T. Knobbe, IEEE Journal on Selected Topics in Quantum Electronics **7**, 567 (2001).
[6] E. McCafferty, Corrosion Science **45,** 1421 (2003).
[7] R. S. Alwitt, H. Uchi, T. R. Beck, R. C. Alkire, Journal of the Electrochemical Society **131,** 13 (1984).
[8] T. Martin, K. R. Hebert, Journal of the Electrochemical Society **148,** B101 (2001).

[9] J. H. Jeong, C. H. Choi, D. N. Lee, Journal of Materials Science **31,** 5811 (1996).
[10] K. Arai, T. Suzuki, T. Atsumi, Journal of the Electrochemical Society **132,** 1667 (1985).
[11] W. Lin, G. Tu, C. F. Lin, Y. M. Peng, Corrosion Science **39,** 1531 (1997).
[12] H. Tsubakino, A. Nogami, Y. Yamamoto, A. Yamamoto, M. Terasawa, T. Mitamura, A. Kinomura, Y. Horino, Applied Surface Science **238,** 464 (2004).
[13] N. Osawa, K. Fukuoka, Corrosion Science **42,** 585 (2000).
[14] F. Mücklich, A. Lasagni, C. Daniel, International Journal of Materials Research **97,** 1337 (2006).
[15] M. D'Alessandria, A. Lasagni, F. Mücklich, Applied Surface Science **255,** 3210 (2008).
[16] L. K. Ang, Y. Y. Lau, R. M. Gilgenbach, H. L. Spindler, Applied Physics Letters **70,** 696 (1997).
[17] K. C. Mills, Y. C. Su, International Materials Reviews **51,** 329 (2006).
[18] M. von Allmen, A. Blatter., Laser Beam Interactions with Materials, Springer, Berlin, 1995.
[19] M. D'Alessandria, F. Mücklich, Applied Physics A: Materials Science and Processing **98,** 311 (2010).
[20] M. Wautelet, Applied Physics A Solids and Surfaces **50,** 131 (1990).
[21] D. Bäuerle, Laser Processing and Chemistry, Springer, 1996.
[22] T. B. Massalki, Binary Alloy Phase Diagrams, Asm International, 1990.
[23] Y. Yu, Ø. Sævik, J. H. Nordlien, K. Nisancioglu, Journal of the Electrochemical Society **152,** B327 (2005).

*Corresponding author: m.paderino@mx.uni-saarland.de